



AXIAL COMPRESSIVE BEHAVIOUR OF HYBRID FRP CONFINED CONCRETE

Filipe Ribeiro¹, José Sena-Cruz², Eduardo Júlio¹ and Fernando G. Branco³

¹ CERIS, Instituto Superior Técnico, Universidade de Lisboa, Portugal;

² ISE, Department of Civil Engineering, University of Minho, Portugal; Email: jsena@civil.uminho.pt;

³ ISE, Department of Civil Engineering, University of Coimbra, Coimbra, Portugal.

ABSTRACT

Fibre Reinforced Polymers (FRP) composites can be effectively used as passive confinement system of concrete columns. Regarding to this option, however, two main drawbacks can be pointed out: (i) in several cases the ultimate lateral strain in the confinement is significantly lower than the tensile strain at failure of the composite, and (ii) the conventional composites experience brittle failure, in an explosive manner in the case of confined concrete without warning which, associated with insufficient residual integrity, requires conservative design. In the present work, different combinations of the following dry unidirectional fabric materials were adopted in materialization of confining systems of concrete cylinders under axial loading: high-modulus carbon, standard carbon and E-glass. From the obtained results it is demonstrated that hybridisation can effectively contribute to maximize the lateral strain efficiency of FRP, exploiting the known hybrid effect of this innovative solution. Furthermore, it also is demonstrated that pseudo-ductile responses are obtained with high-modulus carbon/E-glass combination, which contributes to the elimination of the brittle failure of system. An existing analysis-oriented confinement model in the literature for non-hybrid FRP was satisfactorily modified to predict both: (i) dilation behaviour and (ii) compressive stress-strain behaviour of hybrid confined concrete.

KEYWORDS

New composite materials, systems and strengthening techniques, hybrid effect, pseudo-ductility, confinement.

INTRODUCTION

Fibre Reinforced Polymers (FRP) composites can be effectively used as confinement system of existing concrete columns. It is well known that concrete in compression has a natural tendency to expand laterally (or radially) as damage accumulates due to internal cracking (Pellegrino and Sena-Cruz 2016). The confinement prevents the lateral expansion of cracked concrete, allowing it to achieve higher compressive strength and ultimate axial strain. In this type of applications the level of confining pressure generated by the FRP is dependent on the lateral expansion caused by the concrete (Lim and Ozbakkaloglu 2014a). By default FRP are brittle materials, exhibiting a linear elastic behaviour up to failure. For this reason, when submitted to concentric compression load, the axial stress and strain of the confined concrete continuously increase until the FRP failure. Since there isn't any ductility in confinement material, the assembly failure is abrupt, in an explosive manner, dominated by rupture of the FRP. In this context, unidirectional hybrid FRP composites can be seen as an alternative to traditional FRP composites, since they present pseudo-ductile tensile response - a mechanical non-linear behaviour characterized by flat-topped tensile stress strain curve. However, none of the constituents of the hybrid composites show plastic deformation. Usually, hybrid FRP composites consist of two types of fibres, namely low strain (LS) and high strain (HS) fibres, within the same polymeric matrix. In addition to pseudo-ductility, hybridisation, promotes synergies between the involved reinforcing materials conducting to the increase of the apparent failure strain of LS fibres. This increase in the strain of LS fibres can go up to 50%, e.g. (Ribeiro et al. 2018, Swolfs, Gorbatiikh and Verpoest 2014)), being described in the literature as "hybrid effect".

Over the time, a large number of confinement analytical models have been proposed to predict the behaviour of traditional FRP-confined concrete, e.g. (Ozbakkaloglu, Lim and Vincent 2013). Analysis-oriented models are highlighted because, unlike other types of models, they are capable of establishing all the axial stress-strain behaviour of FRP-confined concrete. They consider the interaction between the confining material and internal concrete core. In these models is assumed that the axial stress and axial strain of FRP-confined concrete are the same as actively confined concrete with a constant confining pressure (equal to that supplied by the FRP) (Lim and Ozbakkaloglu 2014a). In this way, the accuracy of this type of models depends on two input factors (i) lateral strain-axial strain relationship and (ii) stress-strain base curves of the actively confined concrete (Lim and Ozbakkaloglu 2014a). The aim of this research is to assess the performance of 10 different unidirectional (UD) interlayer hybrid composite combinations on the confinement of small-scale plain concrete columns, exploiting the hybrid effect and pseudo-ductility provided by these materials. It was demonstrated that hybrid effect can

maximize the lateral strain efficiency of FRP. Furthermore, an analysis-oriented model is developed to hybrid FRP-confined concrete by modifying the calculation method of the confining pressure in the analysis-oriented model presented in (Lim and Ozbakkaloglu 2014a, Lim and Ozbakkaloglu 2014b).

EXPERIMENTAL PROGRAM

Materials

The concrete used in the present work was supplied by a ready-mixed concrete company, with the following requirements (according to Eurocode 2 (CEN 2004)): (i) strength class C25/30, (ii) exposure class XC2 and (iii) maximum aggregate size of 12.5 mm. Besides, it was required to have a slump class of S4 and chlorides content class Cl0.4, according to the guidelines (IPQ 2005). A value of 160 mm was obtained in the slump test, which is within the range defined for slump class S4 ([160-210] mm), according to the guidelines (IPQ 2005). Twenty eight days after casting, the concrete was characterized by means of compression tests, with 6 cylindrical specimens, in order to obtain the Young's modulus (LNEC 1993) and compressive strength (IPQ 2011): values of 30.79 GPa (CoV = 2.84%) and 33.35 MPa (CoV = 4.33%) were obtained, respectively. During the experimental campaign related with the confined concrete, the concrete age varied between 294 and 315 days. The specimens were kept under standard laboratory conditions until the testing day. In the end of the experimental campaign of the confined cylinders, 3 more plain concrete specimens were tested. Young's modulus (LNEC 1993) and compressive strength (f_{c0}) (IPQ 2011) were obtained equal to 30.29 GPa (CoV = 6.57%) and 33.49 MPa (CoV = 1.33%), respectively.

Three types of dry UD fabric, with a similar areal mass of 400 g/m², were used in this work: (i) UD high-modulus carbon (brand name: S&P C-Sheet 640), (ii) standard carbon (brand name: S&P C-Sheet 240) and (iii) E-glass (brand name: S&P G-sheet E 90/10) denoted as "CHM", "C" and "G", respectively. The comparison of their density, areal mass and thickness properties is presented in Table 1. Experimental mechanical tensile parameters of composite materials made with 1 (1G, 1C and 1CHM) and 3 (3G, 3C and 3CHM) plies of each fabric are as well presented in Table 1. The differences between experimental results obtained in tests with different number of layers are discussed in (Ribeiro et al. 2018). An epoxy-based material (brand name: S&P Resin Epoxy 55) was used as matrix for laminating the studied composites. According to the supplier this epoxy has the following main properties (S&P 2015): (i) a tensile strength of 35.8 MPa; (ii) a strain failure of 2.3%; and, (iii) an elastic modulus of 2.6 GPa.

Table 1 — Properties of the dry fabrics and cured composite materials

| Series ID ⁽¹⁾ | Dry fabric | | | Cured FRP composite properties (Ribeiro et al. 2018) | | |
|--------------------------|-----------------------------|--------------------------------|-------------------------------------|--|----------------------------------|-------------------------------------|
| | Density [g/m ³] | Areal mass [g/m ²] | Nominal thickness, t_f [mm/layer] | Elastic modulus [GPa] (CoV [%]) | Tensile strength [MPa] (CoV [%]) | Strain at the failure [%] (CoV [%]) |
| 1G | 2.60 | 400 | 0.154 | 81.6 (7.39) | 1671.2 (8.59) | 2.31 (3.78) |
| 3G | 2.60 | 400 | 0.154 | 80.6 (10.10) | 1254.8 (15.05) | 2.00 (13.95) |
| 1C | 1.79 | 400 | 0.223 | 231.3 (12.50) | 2565.9 (10.18) | 1.09 (8.81) |
| 3C | 1.79 | 400 | 0.223 | 227.6 (5.80) | 2363.2 (7.44) | 1.02 (6.02) |
| 1CHM | 2.10 | 400 | 0.190 | 624.1 (11.13) | 1749.4 (24.39) | 0.27 (19.61) |
| 3CHM | 2.10 | 400 | 0.190 | 588.2 (3.97) | 1073.9 (18.27) | 0.18 (15.84) |

⁽¹⁾ the number before letters in series is the number of layers.

Test specimens

In the present work, a total of 30 hybrid FRP-confined specimens were prepared and tested under monotonic uniaxial compression. Each specimen was 150 mm in diameter and 300 mm in height. Symmetrical hybrid FRP combinations of 3 and 5 layers were applied as confining material. Wherever possible, LS layers were sandwiched between HS layers. The combinations of 3 symmetrical layers allowed to analyse the following approximate levels of LS fibres vol%: 33% and 66%. In addition, combinations with 5 layers allowed to analyse the following approximate levels of LS fibres vol%: 20%, 40% and 60%. UD fabrics had slightly different thicknesses and, for this reason, the vol% before mentioned was corrected in the next sections, according to the corresponding thickness layer.

Specimen's manufacturing and test setup

Dry fabrics strips of $300 \text{ mm} \times 620 \text{ mm}^2$ used in the confinement of the cylinders were cut from rolls provided by the supplier. The total length allowed an overlap length of 150 mm. The confinement was carried out by hand lay-up method, following the best practices suggested in the guidelines (CNR-DT200 2013). All the specimens were then cured at room temperature for 230 days. Axial deformations of the specimens were measured with 3 linear variable displacement transducers (LVDTs) (range of $\pm 20 \text{ mm}$ and linearity error of $\pm 10\%$), which were mounted equally spaced around the specimen between the loading and supporting steel plates of the 2000 kN loading carrying capacity universal testing machine (UTM), as shown in Figure 1. The lateral strains were measured with 3 or 5 unidirectional strain gauges (one for each layer of fabric) – (TML YEFLA-5-3L with a gauge length of 5 mm). The loading was applied to the specimen through the use of precision-cut high-strength steel disc at a displacement rate of 1.20 mm/min. up to failure.

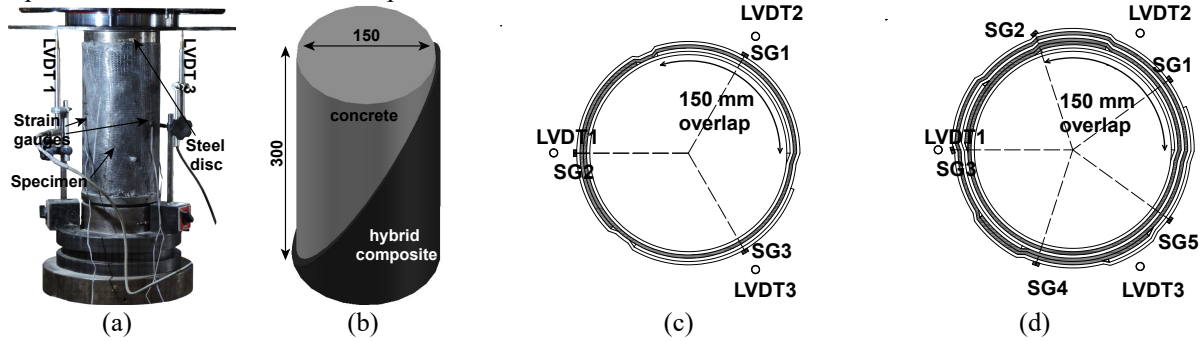


Figure 1: Axial compressive test: (a) illustration of the test; (b) geometry of specimen (dimensions in mm); (c) layers position, LVDT and strain gauge arrangement for confining systems with 3 layers and (d) layers position, LVDT and strain gauge arrangement for confining systems with 5 layers.

ANALYSIS-ORIENTED MODEL

Analysis-oriented models are based on the assumption that for a given confining pressure (f_l), an active confinement model for concrete can be utilized to evaluate a specific point of FRP-confined concrete compressive stress-strain curve. In this way, the complete stress-strain curve of FRP-confined concrete can be obtained by repeating the next incremental procedure until FRP failure:

- i. Lateral strain (ε_l) is the input parameter to estimate the f_l of FRP-confined concrete;
- ii. ε_l and f_l are used to estimate the axial strain (ε_c) of FRP-confined concrete;
- iii. Simultaneously, f_l is used to define the stress-strain model of actively confined concrete;
- iv. The latter allows to determine the compressive stress (f_c) of FRP-confined concrete, assuming that it is equal to the compressive stress of actively confined concrete for the estimated ε_c .

Based on the deformation compatibility between the confining system and the concrete surface, the lateral confining pressure (f_l) applied to concrete by the non-hybrid FRP confining system can be computed according equation (1):

$$f_l = \frac{2E_f t_f \varepsilon_l}{D} \quad (1)$$

where E_f is the elastic modulus of FRP, t_f is the total thickness of FRP and D is the diameter of concrete specimen. In the present work, the exact volume of resin was not directly controlled during the application. For this reason, the total thickness of the FRP was computed considering only the thickness of the dry fabrics, according to the usual practice of the hand lay-up method (CNR-DT200 2013).

For hybrid combinations, f_l was computed assuming a modification of equation (1) as follows:

$$f_l = \frac{2\sigma_h t_f}{D} \quad (2)$$

where σ_h is the stress level of hybrid FRP for a given tensile strain. In this case, it is assumed that tensile strain and lateral strain are the same. The stress level was computed considering an existing tensile stress-strain model in literature (Jalalvand, Czél and Wisnom 2015), as described below.

For each hybrid configuration, three stress levels can be computed (Jalalvand et al. 2015): (i) the stress at which the first crack in the LS material occurs, $\sigma@LF$, (ii) the stress level at which delamination development occurs, $\sigma@del$ and (iii) the stress when the HS material fails, $\sigma@HF$, in accordance with the equations (3) to (5), respectively.

$$\sigma@LF = S_L \frac{\alpha\beta+1}{\alpha(\beta+1)} \quad (3)$$

$$\sigma@del = \frac{1}{1+\beta} \sqrt{\left(\frac{1+\alpha\beta}{\alpha\beta}\right) \left(\frac{2G_{IIc}E_H}{t_H}\right)} \quad (4)$$

$$\sigma@HF = \frac{1}{(1+\beta) K_t m_H \sqrt{V}} S_H \quad (5)$$

where S_L is the reference strength of the LS material, α and β are the modulus and thickness ratios of the LS to HS fibre, G_{IIc} is the mode II interlaminar fracture toughness of the interface between LS layers and HS layers of the hybrid composite, E_H the elastic modulus of the HS fibres, t_H is the half thickness of the HS fibre, m_H is the Weibull strength distribution modulus of the HS fibre, S_H is the reference strength of the HS material, K_t is the stress concentration factor in the high strain material and V is the volume of the specimen.

Knowing the magnitude of all three possible stresses assessed by equations (3) to (5), it is possible to identify one of the four possible damage modes: (i) premature HS failure, (ii) unstable delamination, (iii) LS layer fragmentation and (iv) LS fragmentation and stable delamination. After the determination of the damage modes, it is possible to plot the tensile stress-strain curve of hybrid FRP, as detailed by (Jalalvand et al. 2015).

In the present work, the length and width of the hybrid FRP tensile specimens were assumed equal to $L = 150$ mm and $W = 15$ mm, respectively. The interlaminar toughness, G_{IIc} , for the different hybrid interfaces was judged for each combination in way that, in combinations with experimental pseudo-ductile behaviour, the fragmentation & dispersed delamination damage mode was analytical achieved (see the details in (Ribeiro et al. 2018)). Weibull modulus of HS fibres was assumed equal to $m_H = 29.3$. The value of the stress concentration factor was assumed constant for all of the specimens, $K_t = 0.97$. In these circumstances, the prediction of ε_c based on ε_l of the hybrid or non-hybrid FRP-confined concrete can be estimated according equation (6) (Lim and Ozbakkaloglu 2014a):

$$\varepsilon_c = \frac{\varepsilon_l}{v_i \left[1 + \left(\frac{\varepsilon_l}{v_i \varepsilon_{c0}} \right)^n \right]^{1/n}} + 0.04 \varepsilon_l^{0.7} \left[1 + 21 \left(\frac{f_l}{f_{c0}} \right)^{0.8} \right] \quad (6)$$

where v_i is the initial Poisson's ratio of concrete ($\varepsilon_l/\varepsilon_c$) (Candappa, Sanjayan and Setunge 2001):

$$v_i = 8 \times 10^{-6} f_{c0}^2 + 0.0002 f_{c0} + 0.138 \quad (7)$$

ε_{c0} is the axial strain:

$$\varepsilon_{c0} = (-0.067 f_{c0}^2 + 29.9 f_{c0}' + 1053) \times 10^{-6} \quad (8)$$

n is the curve shape parameter:

$$n = 1 + 0.03 f_{c0} \quad (9)$$

The stress-strain model for actively confined concrete used in the present work is presented in equations (10) and (11) (Lim and Ozbakkaloglu 2014b):

$$f_c = \frac{f_{cc}^* \left(\frac{\varepsilon_c}{\varepsilon_{cc}^*} \right)^r}{r - 1 + \left(\frac{\varepsilon_c}{\varepsilon_{cc}^*} \right)^r}, \text{ if } 0 \leq \varepsilon_c \leq \varepsilon_{cc}^* \quad (10)$$

$$f_c = \frac{f_{cc}^* f_{c,res}}{1 + \left(\frac{\varepsilon_c - \varepsilon_{cc}^*}{\varepsilon_{c,i} - \varepsilon_{cc}^*} \right)^{-2}}, \text{ if } \varepsilon_c > \varepsilon_{cc}^* \quad (11)$$

where f_{cc}^* and ε_{cc}^* are the peak stress and peak strain of actively confined concrete, r is the concrete brittleness (Domingo and Kuang-Han), $f_{c,res}$ is the residual stress (Lim and Ozbakkaloglu 2014b) and $\varepsilon_{c,i}$ is the axial strain corresponding to the inflection point of the descending branch of stress-strain curve (Lim and Ozbakkaloglu 2014b):

$$f_{cc}^* = f_{c0} + 5.2 f_{c0}^{0.91} \left(\frac{f_l}{f_{c0}} \right)^a \text{ where } a = f_{c0}^{-0.06} \quad (12)$$

$$\varepsilon_{cc}^* = \varepsilon_{c0} + 0.045 \left(\frac{f_l}{f_{c0}} \right)^{1.15} \quad (13)$$

$$r = \frac{E_c}{E_c - f_{cc}^* / \varepsilon_{cc}^*} \quad (14)$$

$$f_{c,res} = 1.6 f_{cc}^* \left(\frac{f_l}{f_{c0}} \right)^{0.24} \text{ and } f_{c,res} \leq f_{cc}^* - 0.15 f_{c0} \quad (15)$$

$$\varepsilon_{c,i} = 2.8 \varepsilon_{cc}^* \left(\frac{f_{c,res}}{f_{cc}^*} \right) f_{c0}^{-0.12} + 10 \varepsilon_{cc}^* \left(1 - \frac{f_{c,res}}{f_{cc}^*} \right) f_{c0}^{-0.47} \quad (16)$$

In equation (14), E_c is the elastic modulus of the plain concrete (Lim and Ozbakkaloglu 2014b):

$$E_c = 4400 \sqrt{f_{c0}} \quad (17)$$

RESULTS AND DISCUSSION

The mean values and the coefficient of variation (CoV) of the ultimate conditions of each series of hybrid FRP-confined concrete specimens are presented in Table 2, namely the peak axial stress (f_{cc}) and the peak axial strain (ε_{cc}), the lateral strain at failure of LS fibres, the lateral strain at the peak and the strain reduction factor, k_{ε} , (that

is the ratio between the lateral strain at failure of LS fibres and the tensile strain at failure of LS fibres). Besides, properties of cured hybrid composite materials are presented in same table. From these results it is possible observe that there were 3 combinations with multiple fractures, i.e., in which the failure of LS fibres do not promoted a premature failure of HS fibres: 2G/1CHM/2G, 1G/1CHM/1G, and 1G/1CHM/1G/1CHM/1G. All these combinations have in common the use of the HM carbon fibres. In these cases, catastrophic failures were avoided. However, it has already observed that 1G/1CHM/1G/1CHM/1G combination is in transition failure mode zones and, for this reason, it is expected that there is some random alternation between catastrophic delamination and premature HS fibres failure modes (Ribeiro et al. 2018). It is also possible to observe that there is a tendency to increase the strain reduction factor (k_e) as the volume of LS fibres decreases and the hybrid effect increases. In some cases, the strain reduction factor is superior to 1 which proves that hybridisation allows to completely eliminate the reduction of FRP strain efficiency.

Table 2 — Properties of cured hybrid composite materials and ultimate conditions of hybrid FRP-confined concrete

| Material combination | Series ID ⁽¹⁾ | Volume of LS fibres [%] | Cured hybrid composite properties (Ribeiro et al. 2018) | | | Ultimate conditions of hybrid FRP-confined concrete | | | | k_e at failure of LS fibres |
|----------------------|--------------------------|-------------------------|---|----------------------------------|--|---|-------------------------------|--|------------------------------------|-------------------------------|
| | | | Elastic modulus [GPa] (CoV [%]) | Tensile strength [MPa] (CoV [%]) | Strain at the failure of LS fibres [%] (CoV [%]) | f_{cc} [MPa] (CoV [%]) | ϵ_{cc} [%] (CoV [%]) | ϵ_l at the failure of LS fibres [%] (CoV [%]) | ϵ_l at peak [%] (CoV [%]) | |
| C/G | 1C/1G/1C | 74.3 | 201.7 (9.63) | 2176.9 (8.55) | 1.04 (1.92) | 81.7 (1.48) | 1.23 (6.00) | 0.86 (22.99) | -- | 0.83 |
| | 1G/3C/1G | 68.5 | 202.4 (2.64) | 2216.0 (8.77) | 1.09 (6.26) | 119.4 (2.66) | 2.13 (19.54) | 1.19 (1.35) | -- | 1.09 |
| | 1G/1C/1G/1C/1G | 49.1 | 148.9 (11.75) | 1776.3 (10.55) | 1.19 (3.68) | 108.3 (7.53) | 1.60 (8.27) | 1.29 (12.66) | -- | 1.08 |
| | 1G/1C/1G | 42.0 | 146.7 (5.92) | 1856.0 (5.67) | 1.27 (2.72) | 77.5 (5.00) | 1.23 (12.19) | 1.27 (15.16) | -- | 1.00 |
| | 2G/1C/2G | 26.6 | 110.8 (10.21) | 1244.4 (1.74) | 1.18 (8.27) | 98.3 (2.43) | 1.64 (23.68) | 1.44 (15.90) | -- | 1.22 |
| CHM/G | 1CHM/1G/1CHM | 71.2 | 454.5 (11.95) | 1168.9 (19.49) | 0.26 (11.66) | 54.7 (9.00) | 0.39 (29.22) | 0.21 (46.47) | -- | 0.81 |
| | 1G/3CHM/1G | 64.9 | 439.2 (7.35) | 1053.5 (10.14) | 0.24 (6.43) | 74.5 (6.12) | 0.72 (11.63) | 0.24 (8.31) | -- | 1.04 |
| | 1G/1CHM/1G/1CHM/1G | 45.1 | 318.7 (7.33) | 1105.8 (9.18) | 0.35 (5.02) | 76.6 (1.98) | 0.77 (24.58) | 0.37 (32.84) | 0.90 (4.71) | 1.06 |
| | 1G/1CHM/1G | 38.2 | 252.0 (8.55) | 1054.7 (9.11) | 0.30 (2.39) | 63.7 (1.70) | 0.85 (13.86) | 0.38 (7.71) | 1.27 (14.54) | 1.27 |
| | 2G/1CHM/2G | 23.6 | 214.3 (8.45) | 1164.7 (14.47) | 0.33 (14.65) | 80.5 (3.93) | 1.22 (20.72) | 0.39 (5.96) | 1.49 (9.11) | 1.18 |

⁽¹⁾ The number before letters in series states for the number of layers of each material.

The obtained compressive stress-strain curves are presented in Figure 2 and Figure 3. Some outlier results were ignored. In general, the relationship between uniaxial strain and stress follows approximately a bilinear law, where the slope of the first branch primarily depends on the properties of plain concrete, whereas the slope of the hardening branch is determined by the confining pressures induce by the confining system. This initial phase is similar for all the combinations. From approximately the point corresponding to the theoretical peak of plain concrete (f_{c0} , ϵ_{c0}) – signed in the curves with a dashed line, concrete microcrack propagation occurs and results in a rapid increase in the lateral strain. The different applied confining materials induce different confining pressures which leads to FRP-confined concretes exhibit different trends after f_{c0} , ϵ_{c0} point. It is possible to observe that the higher the modulus of elasticity of FRP, the higher the slope of the second branch. In two cases, in which pseudo-ductile behaviour of the hybrid FRP occurred (Figure 2 (a) and Figure 2 (b)) a flat-topped stress-strain curve is observed.

Analysing the Table 2, it is possible to see the strains at failure of LS fibres were 0.39% and 0.38% and lateral strain at compression stress peak were 1.49% and 1.27% for 2G/1CHM/G and 1G/1CHM/1G combinations, respectively. In this way, the extra strain between the failure point and the strain at failure of LS fibres of the referred to combinations, are 1.10% and 0.89%.

In Figures 2 and 3 the stress-strain curves obtained in the proposed analytical model is also depicted. By comparing these curves with the experimental ones it is possible to conclude that this model is able of predicting the experiments with high accuracy.

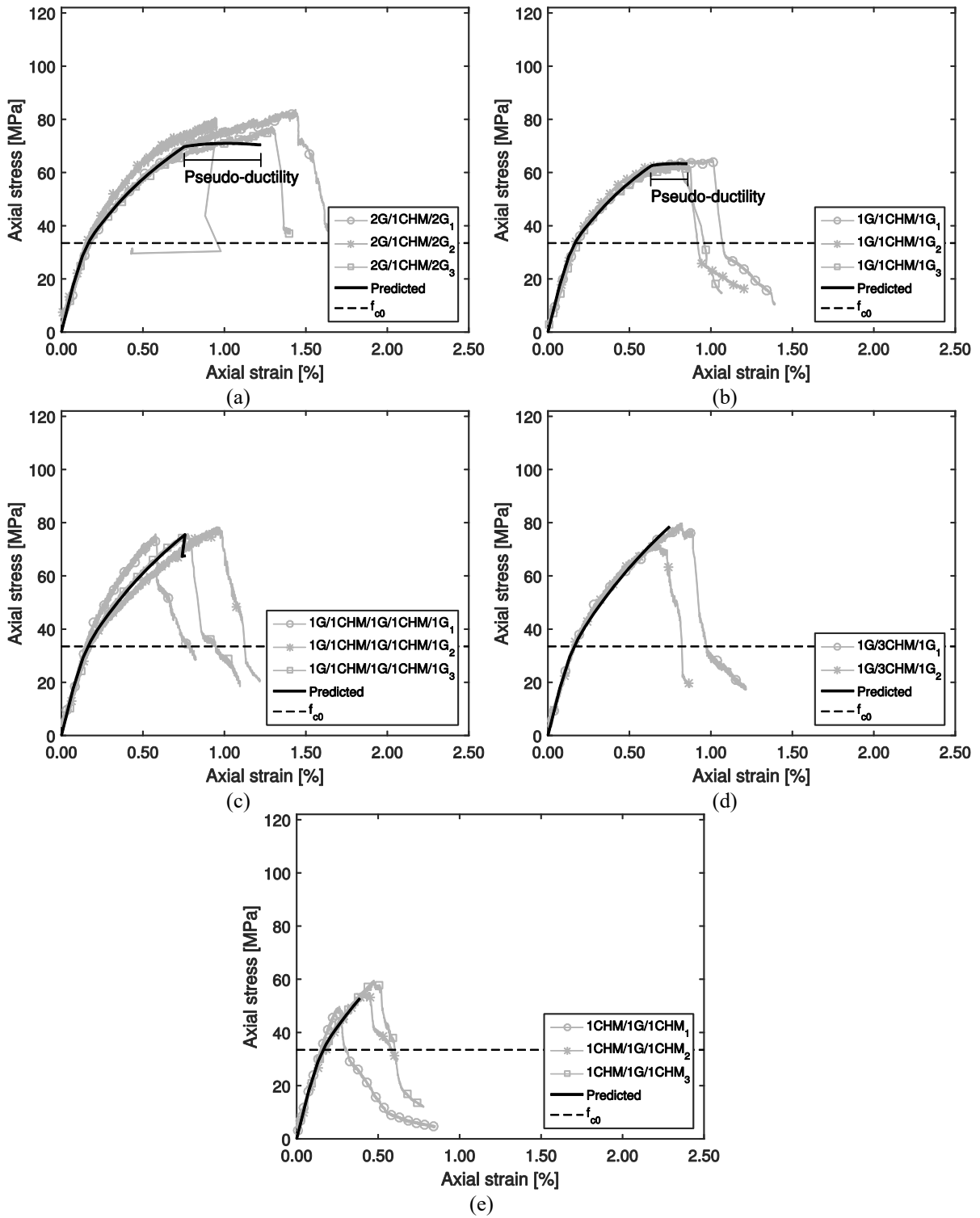


Figure 2: Stress–strain curves of CHM/G combinations: experimental versus predicted values.

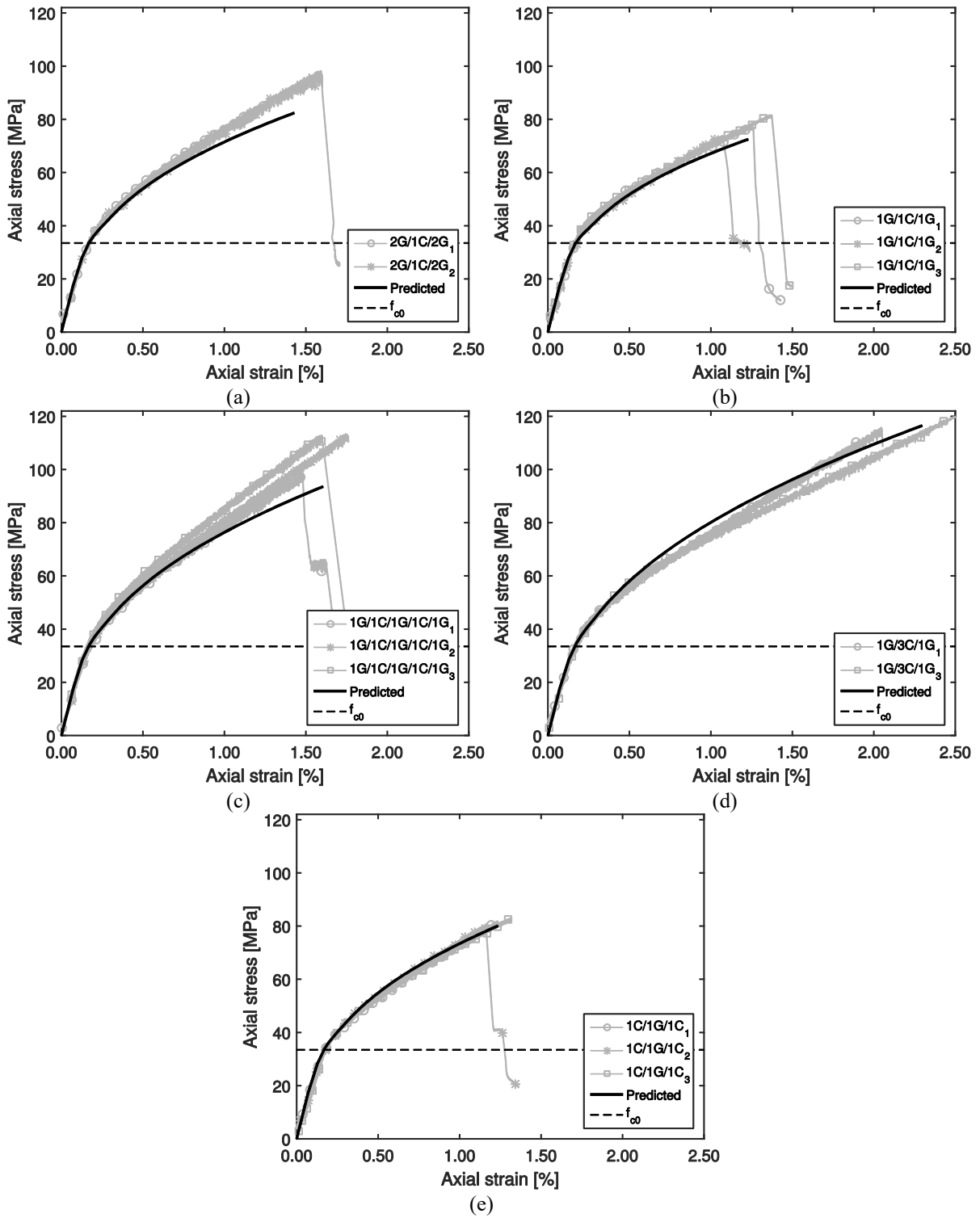


Figure 3: Stress–strain curves of C/G combinations: experimental versus predicted values.

CONCLUSIONS

The compressive behaviour of several hybrid FRP confined small-scale plain concrete columns has been investigated using experimental testing and analytical modelling. All the confining systems were made through the hand layup lamination of three different commercially available dry UD fabrics: HM carbon (CHM), ST carbon (C) and E-glass (G).

It was demonstrated that the common reduction of efficiency of non-hybrid FRP materials can be minimized or even eliminated with hybridisation. It was possible to observe that for large number of hybrid combinations the strain reduction factor was superior to 1. In the two tested hybrid combinations, which included HM carbon as LS material (2G/1CHM/G and 1G/1CHM/1G), pseudo-ductile tensile responses with fragmentation and dispersed delamination of the confining system were achieved. In the compressive stress-strain curves of these combinations a flat-topped stress strain is observed. A mean pseudo-ductile strain of 1.10% and 0.89% for 2G/1CHM/G and 1G/1CHM/1G combination was achieved, respectively. Finally, the presented analysis-oriented confinement model allowed to accurately simulate compressive stress-strain behaviour of all hybrid confined concrete series analysed.

ACKNOWLEDGMENTS

The authors wish to thank to FCT - Portuguese Foundation for Science and Technology and to the Doctoral Program Eco-Construction and Rehabilitation for supporting the PhD scholarship (with the reference PD/BD/52660/2014). Furthermore, this work was partially supported by the following programs: FEDER (European Funds for Regional Development) funds through the Operational Program for Competitiveness Factors – COMPETE, Operational Program for Competitiveness and Internationalization (POCI) and National Funds through FCT under the projects FRPLongDur POCI-01-0145-FEDER-016900 (FCT reference PTDC/ECM-EST/1282/2014) and POCI-01-0145-FEDER-007633. The authors also like to thank to the company S&P Clever Reinforcement Ibérica Lda for the material provided.

REFERENCES

- Candappa, D. C., J. G. Sanjayan & S. Setunge (2001) "Complete Triaxial Stress-Strain Curves of High-Strength Concrete". *Journal of Materials in Civil Engineering*, 13, 209-232.
- CEN (2004) "Eurocode 2: Design of concrete structures. EN 1992-1-1:2004 E, Comité Européen de Normalisation, Bruxelles."
- CNR-DT200 (2013) "Guide for the Design and Construction of Externally Bonded FRP Systems for Strengthening Existing Structures. Advisory Committee on Technical Recommendations for Construction, National Research Council, Rome, Italy".
- Domingo, J. C. & C. Kuang-Han "Stress-Strain Relationship for Plain Concrete in Compression". *Journal Proceedings*, 82.
- IPQ (2005) "Concrete. Part 1: Specification, performance, production and conformity. NP EN 206-1, Portuguese Quality Institute, Lisbon, Portugal."
- IPQ (2011) "Testing hardened concrete. Part 3: Compressive strength of test specimens. EN 12390-3, Portuguese Quality Institute, Lisbon, Portugal."
- Jalalvand, M., G. Czél & M. R. Wisnom (2015) "Damage analysis of pseudo-ductile thin-ply UD hybrid composites – A new analytical method". *Composites: Part A*, 69, 83–93.
- Lim, J. C. & T. Ozbakkaloglu (2014a) "Lateral Strain-to-Axial Strain Relationship of Confined Concrete". *Journal of Structural Engineering*, 141.
- Lim, J. C. & T. Ozbakkaloglu (2014b) "Unified Stress-Strain Model for FRP and Actively Confined Normal-Strength and High-Strength Concrete". *Journal of Composites for Construction*, ASCE, ISSN 1090-0268/04014072 (14).
- LNEC (1993) "Concrete — Determination of the elasticity young modulus under compression. E397-1993, National Laboratory of Civil Engineering, Lisbon, Portugal."
- Ozbakkaloglu, T., J. C. Lim & T. Vincent (2013) "FRP-confined concrete in circular sections: Review and assessment of stress-strain models". *Engineering Structures* 49 1068–1088.
- Pellegrino, C. & J. Sena-Cruz (2016) "Design Procedures for the Use of Composites in Strengthening of Reinforced Concrete Structures". *State-of-the-Art Report of the RILEM Technical Committee 234-DUC*, Springer, ISBN 978-94-017-7335-5.
- Ribeiro, F., J. Sena-Cruz, F. G. Branco & E. Júlio (2018) "Hybrid effect and pseudo-ductile behaviour of unidirectional interlayer hybrid FRP composites for civil engineering applications.". *Construction and Building Materials*, 171, 871-890.
- S&P (2015) "Technical Data Sheet S&P Resin 55".
- Swolfs, Y., L. Gorbatiikh & I. Verpoest (2014) "Fibre hybridisation in polymer composites: a review". *Composites Part A: Applied Science and Manufacturing*, 67, 181-200.